

# Chemically-Sensitive Imaging in Tapping Mode by Chemical Force Microscopy: Relationship between Phase Lag and Adhesion

Aleksandr Noy, Charles H. Sanders, Dmitri V. Vezenov, Stanislaus S. Wong, and Charles M. Lieber\*

Department of Chemistry and Chemical Biology, Harvard University, Cambridge, Massachusetts 02138

Received August 22, 1997. In Final Form: October 20, 1997

Tapping mode atomic force microscopy has been used to record phase-lag images of patterned self-assembled monolayer (SAM) surfaces in alcohol–water solutions using probe tips functionalized with SAMs that terminate in distinct chemical groups. We find that phase contrast between chemically distinct monolayer regions and adhesion forces are directly correlated: increasing adhesion forces lead to increases in the phase lag. Data recorded in alcohol–water mixtures have been analyzed using a driven oscillator model and show that differences in phase shift between distinct regions of the patterned SAMs can be quantitatively related to differences in the work of adhesion,  $W_{st}$ . Because the adhesion forces are readily interpretable on the basis of surface chemical functionality, our results demonstrate that intermittent contact or tapping mode force microscopy can be used to image samples with chemical sensitivity. The implications and potential applications of this new form of chemical force microscopy are discussed.

## Introduction

Force microscopy can provide a wealth of nanometer scale information critical to understanding the properties of surfaces and interfaces.<sup>1–7</sup> For example, contact mode force microscopy has been used to map different domains within heterogeneous samples by sensing variations in local tribological properties,<sup>8</sup> elasticity,<sup>9</sup> and magnetization.<sup>10</sup> In addition, we<sup>11–13</sup> and others<sup>14–17</sup> have shown that it is possible to exploit specific functionalization of probe tips with organic monolayers to discriminate chemically specific forces and image heterogeneous organic layers with chemical sensitivity in organic solvents and aqueous solutions. To date, such chemically sensitive imaging, which we termed chemical force microscopy (CFM),<sup>11</sup> has been carried out in contact mode by recording chemically specific differences in friction. Applications of lateral force-based CFM imaging to softer biological

and polymer samples may, however, be limited since (1) shear forces in contact mode scanning can dominate chemical forces and preclude chemically sensitive imaging and (2) tip-induced deformations that occur in contact mode may also damage samples.

The shear forces present in contact mode imaging can be essentially eliminated by using intermittent contact<sup>18,19</sup> and noncontact<sup>20</sup> oscillation techniques. The intermittent contact or tapping mode technique, in which an oscillating tip taps the surface each oscillation period, is particularly attractive for imaging since it exploits the high-resolution of contact mode while simultaneously minimizing sample deformation. Briefly, when the oscillating tip is brought close to the surface, the oscillation amplitude is reduced from the free amplitude to a new (set point) value that is maintained constant by the feedback loop.

Tapping mode has found widespread application in imaging the structures of biological and polymer samples.<sup>21–26</sup> In several cases, tapping mode has also been shown to provide information about local elastic properties of materials.<sup>27,28</sup> Herein, we describe to our knowledge the first tapping mode studies of chemically heterogeneous organic samples that demonstrate chemically sensitive imaging with this technique. Tapping mode has been used

- (1) Binnig, G.; Quate, C. F.; Gerber, C. *Phys. Rev. Lett.* **1986**, *56*, 930.
- (2) Quate, C. *Surf. Sci.* **1994**, *299/300*, 980.
- (3) Rugar, D.; Hansma, P. *Phys. Today* **1990**, *43*, 23.
- (4) Frommer, J. *Angew. Chem., Int. Ed. Engl.* **1992**, *31*, 1298.
- (5) Lieber, C.; Liu, J.; Sheehan, P. *Angew. Chem., Int. Ed. Engl.* **1996**, *35*, 687.
- (6) Noy, A.; Vezenov, D.; Lieber, C. *Annu. Rev. Mater. Sci.* **1997**, *27*, 381.
- (7) Caprick, R.; Salmeron, M. *Chem. Rev. (Washington, D.C.)* **1997**, *97*, 1163.
- (8) Overney, R. M.; Meyer, E.; Frommer, J.; Guntherodt, H.-J.; Fujihira, M.; Takano, H.; Gotoh, Y. *Langmuir* **1994**, *10*, 1281.
- (9) Maivald, P.; Butt, H.-J.; Gould, S.; Prater, C.; Drake, B.; Gurley, J.; Elings, V.; Hansma, P. *Nanotechnology* **1991**, *2*, 103.
- (10) Rugar, D.; Mamin, H. J.; Guethner, P.; Lambert, S. E.; Stern, J. E.; McFadyen, I.; Yogi, T. *J. Appl. Phys.* **1990**, *68*, 1169.
- (11) Frisbie, C. D.; Rozsnyai, L. F.; Noy, A.; Wrighton, M. S.; Lieber, C. M. *Science* **1994**, *265*, 2071.
- (12) Noy, A.; Frisbie, C. D.; Rozsnyai, L. F.; Wrighton, M. S.; Lieber, C. M. *J. Am. Chem. Soc.* **1995**, *117*, 7943.
- (13) Vezenov, D. V.; Noy, A.; Rozsnyai, L. F.; Lieber, C. M. *J. Am. Chem. Soc.* **1997**, *119*, 2006.
- (14) Green, J.-B. D.; McDermott, M. T.; Porter, M. D.; Siperko, L. M. *J. Phys. Chem.* **1995**, *99*, 10960.
- (15) Sinniah, S. K.; Steel, A. B.; Miller, C. J.; Reutt-Robey, J. E. *J. Am. Chem. Soc.* **1996**, *118*, 8925.
- (16) Williams, J. M.; Han, T.; Beebe, T. P., Jr. *Langmuir* **1996**, *12*, 1291.
- (17) Thomas, R. C.; Houston, J. E.; Crooks, R. M.; Kim, T.; Michalske, T. A. *J. Am. Chem. Soc.* **1995**, *117*, 117.

- (18) Elings, V.; Gurley, J. US Patents Nos. 5412980 and 5519212, 1995.
- (19) Zhong, Q.; Inniss, D.; Kjoller, K.; Elings, V. B. *Surf. Sci.* **1993**, *290*, 1.
- (20) Martin, Y.; Willeams, C.; Wickramasinghe, H. *J. Appl. Phys.* **1987**, *61*, 4723.
- (21) Shao, Z.; Yang, J. *Q. Rev. Biophys.* **1995**, *28*, 195.
- (22) Umamura, K.; Arakawa, H.; Ikai, A. *Jpn. J. Appl. Phys., Part 1* **1993**, *32*, L1711.
- (23) Turner, D. C.; Chunyen, C.; Brandow, S. L.; Murphy, D. B.; Gaber, B. P. *Ultramicroscopy* **1995**, *58*, 425.
- (24) Leula, S. H.; Yang, G.; Robert, C.; Samori, B.; Van Holde, K.; Zlatanova, J.; Bustamante, C. *Proc. Natl. Acad. Sci.* **1994**, *211*.
- (25) Radmacher, M.; Fritz, M.; Hansma, P. K. *Biophys. J.* **1995**, *69*, 264.
- (26) Hansma, H. G.; Laney, D. E.; Bezanilla, M.; Sinsheimer, R. L.; Hansma, P. K. *Biophys. J.* **1995**, *68*, 1672.
- (27) Howard, A. J.; Rye, R. R.; Houston, J. E. *J. Appl. Phys.* **1996**, *79*, 1885.
- (28) Magonov, S. N.; Elings, V. B.; Whangbo, M.-H. *Surf. Sci.* **1997**, *375*, L385.

to record phase-lag images of patterned SAM surfaces using functionalized probe tips in alcohol–water solutions. These data show that the phase contrast between chemically distinct monolayer regions correlates directly with adhesion forces between the tip and sample in these different regions. In addition, fitting these data to a driven oscillator model shows that differences in phase shift between distinct regions of the patterned SAMs can be quantitatively related to differences in the work of adhesion,  $W_{st}$ . Because adhesion forces are readily interpretable on the basis of surface chemical functionality,<sup>6</sup> these studies demonstrate that tapping mode CFM can be used to image samples with chemical sensitivity.

### Experimental Section

Si(100) substrates (Silicon Sense, Nashua, NH) and commercial  $\text{Si}_3\text{N}_4$  tips (Digital Instruments, Santa Barbara, CA) were coated with a 50 Å adhesion layer of Cr followed by 500–1000 Å of Au or Ag.<sup>12</sup> The patterned SAM samples used in our studies were prepared by microcontact ( $\mu\text{C}$ ) printing.<sup>29</sup> Briefly, an elastomeric stamp bearing a pattern of raised and recessed areas was inked with a 1–10 mM ethanolic solution of hexadecanethiol, and then pressed on the metal-coated Si substrate to transfer the pattern. The remaining bare regions of the substrate were subsequently filled with COOH-terminated thiol by covering the sample with a several drops of 16-mercaptohexadecanoic acid. Pattern formation was verified by optical examination of condensation figures.<sup>30</sup> The probe tips were functionalized by immersion in a 1 mM ethanol solution of the appropriate thiol for several hours.

Tapping mode and lateral force images were acquired in fluid solutions using a Nanoscope III atomic force microscope and software (Digital Instruments, Santa Barbara, CA). The tapping mode phase offset was always zeroed before scanning and, therefore, only the relative phase lag was recorded. Phase contrast between two distinct regions of the sample was measured by performing bearing analyses of the phase images. Typically, set point to free amplitude ratios of 0.5–0.8 were used in the experiments.<sup>28</sup> Derivatized probe tips were rinsed with absolute ethanol and dried under a stream of dry  $\text{N}_2$  prior to mounting them in the fluid cell. All images were acquired using 115  $\mu\text{m}$  long and 24  $\mu\text{m}$  wide V-shaped  $\text{Si}_3\text{N}_4$  cantilevers. The spring constants and radii of curvature of these tips were determined from the spectral power density of the thermal resonance<sup>31</sup> and high-resolution electron micrographs, respectively. The spring constants of these cantilevers, 0.1–0.3 N/m are several orders of magnitude lower than those typically used for tapping mode experiments in air, 10–100 N/m.

Our studies were carried out in fluid solution to eliminate contributions from capillary forces that can mask chemical interactions.<sup>11–13</sup> In fluids, the cantilever is driven indirectly via coupling to solution acoustic modes.<sup>32</sup> Recent studies suggest that the observed resonances are due to a convolution of the thermal resonances of the cantilever and the fluid acoustic modes with the latter dominating the observed response.<sup>33</sup> In our studies, we have used the signal at the fluid resonance peak at 9 kHz, since this frequency is closest to the fundamental resonance of our cantilevers.<sup>34</sup> This frequency choice allows us to maintain high sensitivity, while keeping the drive amplitude at a reasonable level (typically 100–150 nm).

### Results and Discussion

**Imaging of Patterned SAMs in Ethanol.** The patterned SAMs produced by  $\mu\text{C}$  printing were made using alkanethiols that have the same lengths and differ only

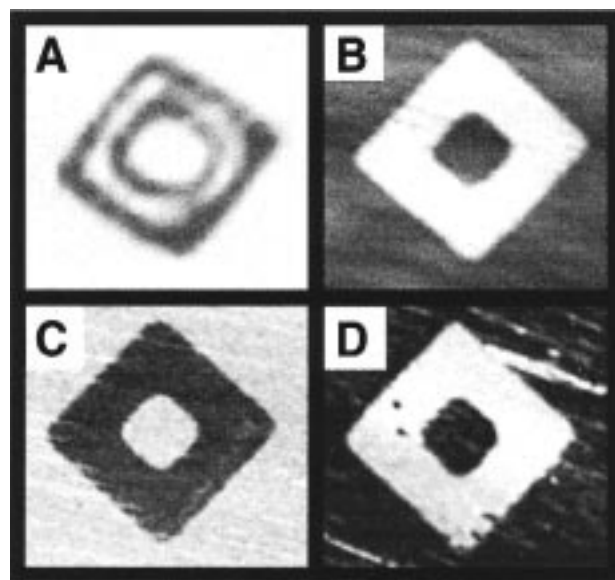


**Figure 1.** (A) Condensation figure obtained for a patterned self-assembled monolayer with  $\text{CH}_3$ - and  $\text{COOH}$ -terminated regions. Water droplets condense on the  $\text{COOH}$ -terminated regions and appear as a dark ring in this optical micrograph. (B) Friction map of a similar size area obtained with a  $\text{COOH}$ -terminated tip. Light and dark areas correspond to the regions of high and low friction, respectively. (C, D) Phase lag maps of the same sample taken with (C) a  $\text{COOH}$ -terminated tip and (D) a  $\text{CH}_3$ -terminated tip. Darker regions correspond to greater phase lag. The images were recorded at a scan rate of 2 Hz and cantilever free oscillation amplitude of  $100 \pm 10$  nm (root mean square). All images are  $25 \mu\text{m} \times 25 \mu\text{m}$ . The contrasts in (B) and (C) and (D) correspond to friction differences of  $\sim 25$  nN and phase variations of 9 and  $4^\circ$ , respectively.

in the functionality of the terminal surface carbon; that is,  $\text{HS}-(\text{CH}_2)_{15}-\text{R}$ , where R = methyl ( $\text{CH}_3$ ) or carboxyl ( $\text{COOH}$ ). Hence, these patterned surfaces are ideal systems to explore the contributions of chemical interactions to tapping mode images, since the equal chain length alkanethiols yield SAM samples that are topographically flat and have uniform elastic properties.

An optical condensation image highlighting the  $\text{COOH}$ - and  $\text{CH}_3$ -terminated regions of a patterned SAM sample is shown in the Figure 1A. Water droplets condense on the hydrophilic  $\text{COOH}$ -terminated regions of the sample and appear as a ring-shaped object. A lateral force image of a similar size region of a clean patterned substrate acquired in ethanol with a  $\text{COOH}$ -functionalized tip is shown in Figure 1B. The  $\text{COOH}$ -terminated regions of the sample exhibit higher friction than  $\text{CH}_3$ -terminated regions as expected for the stronger  $\text{COOH}/\text{COOH}$  versus  $\text{CH}_3/\text{COOH}$  interaction.<sup>12</sup> These results are also in agreement with our previous measurements on samples patterned by photolithography.<sup>11,12</sup> A corresponding phase lag image of the same area obtained with a  $\text{COOH}$ -terminated tip in tapping mode is presented in Figure 1C. It is evident from this image that the phase lag is sensitive to differences in tip–sample interactions: the square ring corresponding to the area of  $\text{COOH}/\text{COOH}$  sample–tip interaction has a larger phase lag (appears darker) than surrounding regions where the interaction ( $\text{CH}_3/\text{COOH}$ ) is weaker. Although the phase lag and friction images appear to have opposite contrast, this is simply due to the sign convention in tapping mode: increasing phase lag is indicated by increasing darkness, while increasing friction is indicated by increasing brightness. The same phase contrast was observed reproducibly for a number of independent samples and functionalized tips, and hence

(29) Kumar, A.; Biebuyck, H.; Whitesides, G. *Langmuir* **1994**, *10*, 1498.

(30) Lopez, G.; Biebuyck, H.; Frisbie, C.; Whitesides, G. *Science* **1993**, *260*, 647.

(31) Hutter, J. L.; Bechhoefer, J. *Rev. Sci. Instrum.* **1993**, *64*, 1868.

(32) Putman, C.; van der Werf, K.; DeGroot, B.; van Hulst, N.; Greve, J. *Appl. Phys. Lett.* **1994**, *64*, 2454.

(33) Schaffer, T.; Cleveland, J.; Ohnesorge, F.; Walters, D.; Hansma, P. *J. Appl. Phys.* **1996**, *80*, 3622.

(34) Cleveland, J. Personal communication.

we conclude that it is representative of the intrinsic interactions between the functionalized samples and tips.

To test further our suggestion that the phase contrast observed with the COOH-terminated tip is due to difference in the chemical interactions between the sample and tip, we have imaged the patterned sample using a CH<sub>3</sub>-terminated tip. Previously, we showed that a change in the tip functionality leads to a contrast reversal in lateral force images.<sup>11,12</sup> The inversion in friction contrast was predictable on the basis of strengths of the different sample–tip interactions determined from adhesion measurements; that is, COOH/COOH > CH<sub>3</sub>/CH<sub>3</sub> > CH<sub>3</sub>/COOH in ethanol. Significantly, tapping mode images acquired with CH<sub>3</sub>-terminated tips also show an inversion in the phase contrast (Figure 1C): the CH<sub>3</sub>-terminated regions of the sample that interact more strongly with the CH<sub>3</sub>-terminated tip than the COOH-terminated regions of the sample have a greater phase lag. These data thus demonstrate that tapping mode phase lag imaging can be used to map functional group distributions in a predictable way.

**Tip–Sample Adhesion and Phase Lag.** To understand further these new results we have considered a simple oscillator model. Following Magonov et al., the phase angle of a driven cantilever can be expressed as:<sup>28</sup>

$$\Phi = \tan^{-1} \left( \frac{m\omega\omega_0}{Q(k - m\omega^2)} \right) \quad (1)$$

where  $k$ ,  $Q$ ,  $m$ ,  $\omega_0$ , and  $\omega$  are cantilever spring constant, quality factor, mass, resonance frequency, and the driving frequency, respectively. In the presence of tip–sample interactions, the force constant of the cantilever is modified to reflect the interaction stiffness. In this case, the phase angle is given by

$$\Phi = \tan^{-1} \left( \frac{m\omega\omega_0}{Q(k + \sigma - m\omega^2)} \right) \quad (2)$$

where  $\sigma$  is the sum of force derivatives for these interactions. For  $\sigma \ll k$  the phase angle shift  $\Delta\Phi_0$  between the free and interacting cantilever can be written as<sup>28</sup>

$$\Delta\Phi_0 \propto Q\sigma/k \quad (3)$$

This formula predicts negative phase shift (i.e., greater phase lag) when the force acting on the tip is attractive. Therefore, the regions of the sample that interact more strongly with the tip will appear darker (greater phase lag) on the phase map.

Recently, this model has been used to analyze phase contrast images of polyethylene and poly(diethylsiloxane) samples acquired with stiff Si tips in air.<sup>28</sup> The phase shifts were interpreted in terms of repulsive tip–sample interactions reflecting differences in the Young's moduli of the two materials. Although the set point to free amplitude ratios used in our experiments, 0.5 to 0.8, overlap somewhat with those used in this previous work, the much softer cantilevers used in our fluid solution studies ( $k = 0.1$ – $0.3$  N/m versus  $k = 10$ – $100$  N/m in air) effectively reduce the role of elastic deformations of the sample and shift the imaging regime to that of light tapping.

We have extended this model to our system as follows. First, because the different regions of patterned samples have identical chain lengths and structure, we assume that mechanical interactions are unimportant. Second, we assume that the interaction stiffness  $\sigma$  is proportional

to the work of adhesion,  $W_{st}$ , between the sample and tip.  $W_{st}$  is known to be a major factor determining the magnitude of tip–surface interactions,<sup>12,35</sup> and thus we expect that it also plays an important role in determining phase lag contrast. With these two assumptions, the phase contrast between two chemically distinct regions of the sample can be expressed as

$$\Delta\Phi \frac{k}{Q} \propto \Delta W_{st} \quad (4)$$

where  $\Delta W_{st}$  is the difference between the work of adhesion for the tip interacting with the two chemically distinct sample regions. Therefore, the phase contrast is expected to be proportional to the differences in the interaction energies.

**Phase Contrast in H<sub>2</sub>O/Methanol Solvent Mixtures.** To investigate experimentally the quantitative relationship between adhesive interactions and phase contrast, we have imaged CH<sub>3</sub>–COOH patterned SAM samples with CH<sub>3</sub>-terminated tips in a series of methanol/water mixtures. Increases in the water content produce systematic changes in the solid–liquid surface free energies that determine  $W_{st}$ .<sup>13</sup> For example, as the percentage water increases from 20 to 60 to 80%,  $W_{st}$ –(CH<sub>3</sub>/CH<sub>3</sub>) and  $W_{st}$ –(COOH/CH<sub>3</sub>) increase from 15.2 and 2.2 mJ/m<sup>2</sup> to 35.2 and 4.9 mJ/m<sup>2</sup> to 70.4 and 20.6 mJ/m<sup>2</sup>, respectively.<sup>36</sup> Therefore, the interaction strength varies systematically with solvent composition, while other parameters of the system remain constant.

Significantly, the phase lag images recorded on the CH<sub>3</sub>–COOH patterned SAM samples with CH<sub>3</sub>-terminated tips show systematic changes in phase contrast with increasing amounts of water (Figure 2). As the percentage of water increases from 0 to 80%, we find that the phase contrast increases with the CH<sub>3</sub>/CH<sub>3</sub> interaction exhibiting increasingly larger phase lag. These results are thus in qualitative agreement with our expectations, since the  $W_{st}$  values determined from our adhesion measurements show that  $W_{st}$ –(CH<sub>3</sub>/CH<sub>3</sub>) increases more rapidly than  $W_{st}$ –(COOH/CH<sub>3</sub>) with increasing percentage of water.

We have also examined the quantitative agreement of our results with the simple model presented above by plotting the phase contrast versus  $\Delta W_{st}$  (Figure 3). The phase contrast data were multiplied by the cantilever spring constant and divided by a cantilever quality factor to eliminate cantilever dependence, in accordance with eq 4. This figure summarizes phase lag imaging results and adhesion measurements made for nine different methanol/water solvent compositions. Significantly, the data presented in Figure 3 confirm that phase lag contrast increases linearly with increasing differences in the sample–tip interaction energy. Moreover, the linear fit through these data intersects the origin (within experimental error) and thus suggests that our model, which attributes phase contrast solely to differences in  $W_{st}$ , provides a good description of the origin of phase contrast in these monolayer systems.<sup>37</sup> Alternatively, if the adhesion data for different surface components is available for several solvents, the plot of phase contrast versus the interaction free energy difference (such as presented in

(35) Johnson, K. L. *Proc. R. Soc. London, Ser. A* **1997**, 453, 163.

(36) Vezenov, D. V.; Zhuk, A. V.; Noy, A.; Lieber, C. M. Manuscript in preparation.

(37) This model assumes that the cantilever is driven at its resonance frequency, although in our experiments the cantilever was driven at the fluid mode closest to this resonance. Therefore, the model should be considered as an approximate description of the real system.

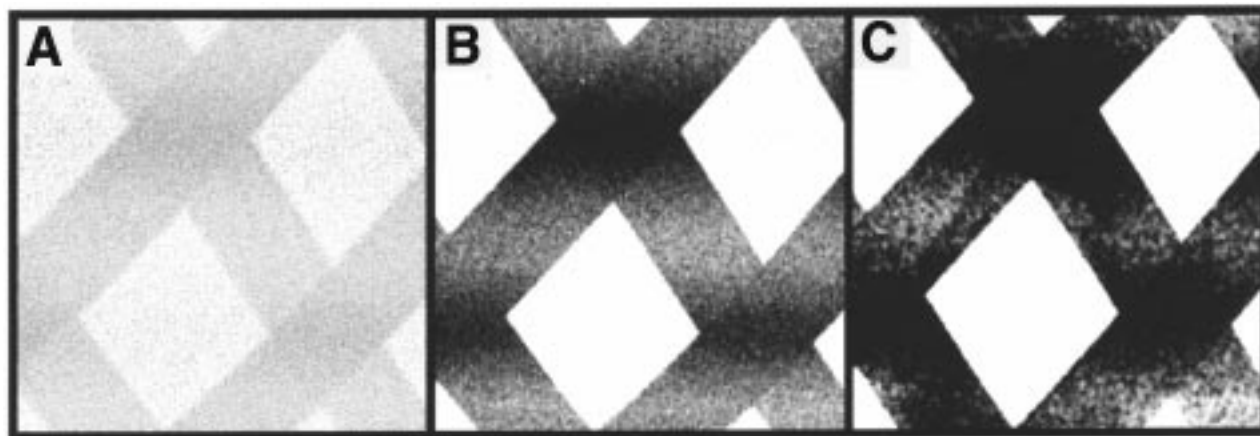


**Figure 2.** Phase lag maps of a SAM sample patterned with COOH-terminated square regions surrounded by a CH<sub>3</sub>-terminated background recorded with the same CH<sub>3</sub>-terminated tip in a series of methanol–water solvents. The water content, phase contrast, and differences in tip–sample work of adhesion are (A) 20%, 16° and 12.9 mJ/m<sup>2</sup>, (B) 60%, 32°, and 30.3 mJ/m<sup>2</sup>, and (C) 80%, 50°, and 49.8 mJ/m<sup>2</sup>. The gray scale in each of these 25 μm × 25 μm images represents phase variation of 50°. The imaging set point to the free amplitude ratio was maintained at 0.60 ± 0.05. The square pattern in the images was elongated along slow scan axis due to elastic recovery of the O-ring seal of the fluid cell.

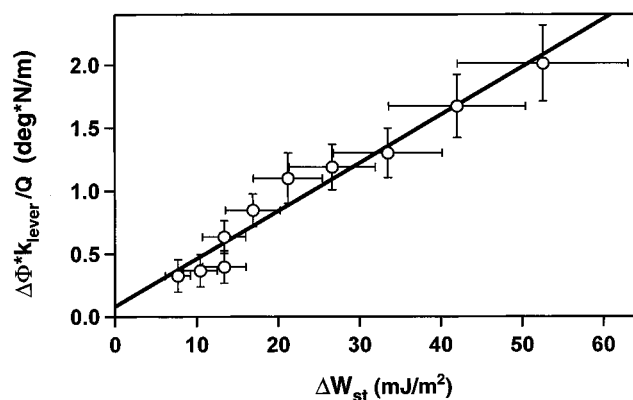


**Figure 3.** Plot of the product of the cantilever spring constant and phase contrast divided by the cantilever quality factor versus the difference in tip–sample interaction free energies for the two distinct sample regions shown in Figure 2. The data were obtained with increasing percentage water from 0 to 80%. The straight line is a linear fit to the data. The plot combines data obtained with two cantilevers with different spring constants and quality factors ( $k_1 = 0.14$  N/m,  $Q_1 = 3.43$  and  $k_2 = 0.36$  N/m,  $Q_2 = 4.14$ ). Both cantilevers had tips terminating in CH<sub>3</sub> groups. Error bars represent standard deviations determined by bearing analysis of phase lag images and errors in work of adhesion values originating from uncertainties in the tip radii.

Figure 3) can be used to evaluate relative contributions of the viscoelastic and chemical factors.

### Conclusions

In summary, we have shown that tapping mode phase lag imaging is sensitive to the adhesive interactions between samples and tips. Using chemically modified probes to image patterned SAM surfaces, we have shown that the phase lag images map qualitatively and quantitatively the magnitude of the tip–surface interaction in the absence of large sample stiffness variations. Specifically, phase contrast and adhesion data recorded in

methanol–water mixtures were analyzed using a driven oscillator model and show that differences in phase lag between distinct regions of the patterned SAMs can be quantitatively related to differences in the work of adhesion,  $W_{st}$ . Because the adhesion forces are readily interpretable on the basis of the surface chemical functionality, these new results demonstrate that phase imaging with modified AFM probes represents a viable strategy for chemically sensitive mapping of functional group distributions on surfaces and thus extends the previous concept of chemical force microscopy.

In addition, we believe that these studies have important implications for several areas. Specifically, this work suggests that it should be possible to use phase lag imaging with chemically modified tips to map domains of different chemical functionality on polymer surfaces, to identify residual contaminants resulting from, for example, semiconductor processing, and to image biological sample surfaces with chemical sensitivity. To realize these applications, it will be necessary, however, to control the tapping conditions such that mechanical and chemical contributions to the phase signal are minimized and maximized, respectively. We believe that this can be achieved with light tapping and are currently testing these ideas in diblock polymer systems.

**Acknowledgment.** C.M.L. acknowledges discussions with V. Elings that motivated this work. We also acknowledge discussions during the course of these studies with J. Cleveland, S. Magonov, C. Prater, and V. Elings. C.M.L. thanks the Air Force Office of Scientific Research (F49620-97-1-0005) for generous support of this work, and Digital Instruments, Inc., for donation of equipment critical to the completion of these experiments. S.S.W. acknowledges fellowship support from the Fonds pour la Formation de Chercheurs et l'Aide à la Recherche (Québec, Canada).

LA970948F